Nuclear Medicine & Biology, Vol. 24, pp. 275–286, 1997

ISSN 0969-8051/97/$17.00 + 0.00
PII S0969-8051(97)00039-5

PET-Pharmacokinetics of ^{18}F-Octreotide: A Comparison with ^{67}Ga-DFO- and ^{86}Y-DTPA-Octreotide

Hans-Jürgen Wester,[1] Jörg Brockmann,[1] Frank Rösch,[1] Walter Wutz,[1] Hans Herzog,[2] Peter Smith-Jones,[3] Barbara Stolz,[3] Christian Bruns[3] and Gerhard Stöcklin[1]

[1]INSTITUTE FÜR NUKLEARCHEMIE UND [2]MEDIZIN, KFA JÜLICH, GERMANY, AND [3]PRECLINICAL RESEARCH, SANDOZ LIMITED, BASEL, SWITZERLAND

ABSTRACT. The quantitative uptake kinetics of (2-[^{18}F]fluoropropionyl-(D)phe^1)-octreotide (I), a somatostatin (SRIF) receptor-specific tracer, was measured by PET. Conventional organ biodistribution and *in vivo* stabilities of the tracer as well as *in vivo* displacement and SRIF receptor blocking were determined. The ^{18}F-fluorinated octreotide was compared with ([^{67}Ga]-DFO-B-succinyl-(D)phe^1)-octreotide (II) and ([^{86}Y]-DTPA-(D)phe^1)-octreotide (III). Initially, 2–10 MBq of the labeled tracers were injected into male Lewis rats bearing an exocrine pancreatic islet cell tumor. PET measurements were performed dynamically between 0 and 120 min postinjection. Organ distributions were determined 5, 15, 30, 60, and 120 min postinjection. The extent of metabolic degradation was analyzed in serial blood and urine samples as well as in homogenized samples of tumor, liver, and kidney. The uptake of (I) by the tumor was rapid (maximum accumulation at 1–2 min postinjection) and high (about 0.5 ± 0.2 %ID/g), followed by a fast and continuous release with $k_{off} = 10 \pm 2 \cdot 10^{-5}$ s^{-1}. The tracer was found to remain intact *in vivo* up to 120 min postinjection. Specific binding of (I) to SRIF receptors in the adrenals, the pancreas, and the pituitary gland was demonstrated *in vivo* by pretreatment and displacement experiments. Compound (II) also showed a fast uptake by the tumor. Its tumor residence half-life was longer ($k_{off} = 3.0 \pm 0.5 \cdot 10^{-5}$ s^{-1}). Compound (II) was also predominantly excreted intact. One hour postinjection, the remaining activity in the blood pool was found to be bound to serum proteins. Early uptake kinetics for compound (III) were also rapid but reached only half the tumor uptake of (II). Compared to (I), the release of ^{86}Y-activity from the tumor was slower ($k_{off} = 3.1 \pm 1.3 \cdot 10^{-5}$ s^{-1}). Compared to (II), compound (III) was considerably less stable *in vivo*. The main critical organs for (II) and (III) are kidneys and bones, whereas (I) is predominantly accumulated in the liver. The *in vivo* behavior of (I) closely resembles ^{14}C-labeled octreotide. Thus, ^{18}F-labeled octreotide may be of interest in the quantitation and investigation of *in vivo* properties of somatostatin receptors by PET. However, the short residence of (2-[^{18}F]fluoropropionyl-(D)phe^1)-octreotide in tumors and its hepatobiliary excretion may complicate the interpretation of abdominal tumors. NUCL MED BIOL 24;4:275–286, 1997.

KEY WORDS. Somatostatin receptors, Octreotide, Fluorine-18, Gallium-67, Yttrium-86

INTRODUCTION

In vivo detection of SRIF (somatotropin release inhibiting factor) receptor-positive tumors using radiolabeled somatostatin analogues such as the octapeptide octreotide (Sandostatin®, SDZ 201-995) is a tool routinely used in tumor diagnosis (25). For this purpose, various somatostatin-derived radiopharmaceuticals have been developed, such as Octreoscan®111 (([^{111}In]-DTPA-(D)phe^1)-octreotide (SDZ 215-811)) (4), [^{123}I]-Tyr^3-octreotide (SDZ 204-090) (5), ([^{99m}Tc]-PnAO-(D)phe^1)-octreotide (SDZ 219-387) (27), and [^{99m}Tc]-N$_4$-Bz-octreotide (SDZ 220-778) (44) for SPET as well as ([^{68}Ga]-DFO-B-succinyl-(D)phe^1)-octreotide (42) and [^{64}Cu]-TETA-(D)phe^1)-octreotide (3) for PET. Among these tracers, ([^{111}In]-DTPA-(D)phe^1)-octreotide and [^{123}I]-Tyr^3-octreotide are in routine clinical application (23, 24). Additionally, some radiolabeled analogues of the synthetic octapeptides RC-121, RC-160, and RC-161 have been reported and seem to have some potential as tracers for somatostatin receptor imaging (7, 9, 10, 43).

The possibility of dynamic quantification, dosimetric calculations, and the measurement of fast *in vivo* kinetics together with the higher resolution may favor the use of PET and positron-emitting radionuclides (such as ^{18}F, ^{68}Ga, ^{86}Y, and ^{64}Cu). Recently, the synthesis of (2-[^{18}F]fluoropropionyl-[D]phe^1)-octreotide has been described (17) as a potential tracer for *in vivo* quantitation of SRIF receptors. The aim of the present study was to evaluate the potential of ^{18}F-octreotide for *in vivo* tumor diagnosis with PET by characterizing its quantitative uptake and binding kinetics and the extent of *in vivo* degradation in rats bearing an exocrine pancreatic tumor.

To compare the results with other octreotide derivatives suitable for PET, similar measurements were carried out for ([^{67}Ga]-DFO-B-succinyl-(D)phe^1)-octreotide and ([^{86}Y]-DTPA-(D)phe^1)-octreotide (Fig. 1), which was prepared as an yttrium-86-analogue of Octreoscan® (SDZ 215-811). For the latter compound, however, the main intention was to determine the quantitative uptake kinetics as a prerequistite to calculate dosimetric data using yttrium-86 ($t_{1/2}$ = 14.7 h, 32% β^+) and PET. These data are relevant for the evaluation of SRIF receptor-positive tumors with yttrium-90 ($t_{1/2}$ = 64.1 h, 100% β^-)-labeled somatostatin analogues.

Address reprint requests to: H.-J. Wester, Klinik für Nuklearmedizin, TU München, Ismaningerstr. 22, D-81675 München, Germany.
Received 27 December 1995.
Accepted 10 May 1996.

TABLE 1. Summary of Animal Experiments (Male Lewis Rats Bearing an Exocrine Pancreatic Tumor)

Octreotide derivative	Animals	Injected activity [μCi]	Injected peptide concentration [nmol]	Animal studies
[^{18}F]-octreotide	F1	218	0.5	PET 0–120 min
	F2	218	0.5	PET 0–120 min
	F3	16.5	0.16	PET 0–120 min
	F4–15	5–25	0.01–0.06	*ex vivo* biodistribution
[^{67}Ga]-octreotide	G1–15	8.5	0.4	*ex vivo* biodistribution
[^{86}Y]-octreotide	Y1	107	0.29	PET 0–120 min
	Y2	98	0.29	PET 0–60 min
	Ye–15	50–63	0.14	*ex vivo* biodistribution

MATERIALS AND METHODS

Instrumentation

HPLC of ^{18}F-octreotide was carried out with a system consisting of two pumps (L6000 and L6200A intelligent pump, both Merck-Hitachi, Darmstadt, Germany). The recorded data were processed by a Ramona software system (Nuclear Interface, Datentechnik für Strahlenmeßgeräte GmbH, Münster, Germany). HPLC of the metal-labeled compounds was performed with a SYKAM S1020 system (Sykam GmbH, Gilching, Germany) coupled to a 486/50 PC operating AXXIOM software system. For continuous radioactivity measurement, the outlet of the UV-photometer was connected to a NaI(Tl) well-type scintillation counter (Meßelektronik Dresden GmbH, Dresden, Germany).

Reagents

All chemicals were obtained commercially and were of analytical grade unless stated otherwise. Both ε-Boc-Lys^5-octreotide and [Desferrioxamine B-succinyl-(D)phe^1]-octreotide (DFO-octreotide) were obtained from Sandoz Pharma, Basel, Switzerland. (Diethylenetriamine *N,N,N′,N″*-tetraacetic acid-*N″*-acetyl-(D)phe^1)-octreotide (DTPA-octreotide) was prepared by reaction of DTPA-bisanhydride with ε-Boc-Lys^5-octreotide and subsequent deprotection of the lysine group (4).

Radioisotopes

No-carrier added (n.c.a.) fluorine-18 ($t_{1/2}$ = 109.7 min, 98% β^+) was produced via the ^{18}O(p,n)^{18}F nuclear reaction by bombardment of an isotopically enriched [^{18}O]water target with a 17-MeV proton beam at the BC 1710 cyclotron (JSW), as described previously (18). Gallium-67 ($t_{1/2}$ = 78.3 h, EC) was obtained from Amersham as gallium citrate. Anion exchange column chromatography removed the excess citrate. Yttrium-86 ($t_{1/2}$ = 14.74 h, 33% β^+) was produced at the Jülich CV28 compact cyclotron via the ^{86}Sr(p,n)-reaction on highly enriched $^{86}SrCO_3$ (36, 37). After the chemical separation, isotopically pure (>97%) stock solutions of n.c.a. ^{86}Y(III) in 0.1 M HCl were obtained with a specific volume activity of >10 mCi/mL. For some conventional biodistribution measurements, the longer-lived γ-emitter yttrium-88 ($t_{1/2}$ = 106.6 days, EC) was used. This isotope was produced via the ^{nat}Sr(p,xn)-reaction at the Jülich CV28 compact cyclotron in the same way as described for the ^{86}Sr(p,n)^{86}Y-system.

Radiopharmaceuticals

The (2-[^{18}F]fluoropropionyl-(D)phe^1)-octreotide was synthesized in a three-step procedure (17). ([^{67}Ga]-DFO-B-succinyl-(D)phe^1)-octreotide was prepared by addition of 260 μCi ^{67}Ga(III) in 3 mL 0.1 M NH_4OAc (pH 5) to 60 μL of a DFO-(D)phe^1-octreotide stock solution (0.19 mM) and subsequent incubation at room temperature (RT) for 20 min according to a previously published report (42). DTPA-(D)phe^1-octreotide was labeled with yttrium-86 by addition of 6 μL of a DTPA-(D)phe^1-octreotide stock solution (0.18 mM) to 500 μCi (18.5 MBq) $^{86}YCl_3$ in 1 mL 0.01 M Na_3Cit (pH 5.9) and incubation at RT for 15 min.

Quality Control

Final determination of specific activity and radiochemical purity was performed by HPLC using the following conditions: (2-[^{18}F]fluoropropionyl-(D)phe^1)-octreotide: LiChrospher RP-18 Select B, 5 μm, 125 × 8 mm, gradient system: eluant A = water/acetonitrile/phosphoric acid 900/100/6; v/v/v), then adjusted to pH 2.9; eluant B = Water/acetonitrile (300/700; v/v); gradient: 5%–95% B in 20 min, flow rate = 2.5 mL/min, T = 20°C; k′ = 5.5. ([^{67}Ga]-DFO-B-succinyl-(D)phe^1)-octreotide: Chromasil C-18 peek, 5 μm, 250 × 4 mm; gradient system: eluant A = 0.1% acetic acid; eluant B = acetonitrile; gradient: 2% B const. 0–3 min; 2%–30% B 3–5 min; 30%–35% B 5–20 min, 35%–100% B 20–25 min, flow rate = 1.0 mL/min, T = 20°C; k′ = 8.4). ([^{86}Y]-DTPA-(D)phe^1)-octreotide: Chromasil C-18 peek, 5 μm, 250 × 4 mm; gradient system: eluant A = 0.05 M sodium acetate,

TABLE 2. *Ex Vivo* Biodistribution Data of (2-[^{18}F]Fluoropropionyl-(D)phe^1)-Octreotide in Rats Bearing an Exocrine Pancreatic Islet Cell Tumor and Control Rats, 60 and 120 min Postinjection

	Tumor-Bearing Rats		Control Rats	
Organ	60 min	120 min	60 min	120 min (n = 1)
Pituitary	0.71 ± 0.03	0.69 ± 0.37	1.27 ± 0.21	1.42
Brain	0.01 ± 0.01	0.01 ± 0.01	0.01 ± 0.01	0.01
Bone	0.04 ± 0.01	0.05 ± 0.01	0.17 ± 0.14	0.03
Intestines	1.90 ± 0.34	1.79 ± 0.24	6.30 ± 2.41*	2.57
Pancreas	0.70 ± 0.08	0.34 ± 0.01	1.12 ± 0.41	0.67
Liver	1.23 ± 0.04	1.63 ± 1.41	1.93 ± 0.29	1.11
Blood	0.10 ± 0.03	0.04 ± 0.01	0.12 ± 0.03	0.06
Kidney	1.30 ± 0.13	0.59 ± 0.21	1.04 ± 0.22	1.50
Adrenals	2.40 ± 0.48	1.07 ± 0.38	2.18 ± 0.27	1.71
Heart	0.06 ± 0.01	0.02 ± 0.01	0.07 ± 0.02	0.04
Lung	0.14 ± 0.01	0.06 ± 0.01	0.19 ± 0.03	0.09
Tumor	0.52 ± 0.24	0.17 ± 0.02	—	—
Spleen	0.21 ± 0.05	0.11 ± 0.02	0.14 ± 0.04	0.07

(n = 3, unless stated otherwise). Calculated data expressed as %injected dose/g (mean ± SD).
*Only parts of the intestines were counted.

adjusted to pH 5.5; eluant B = methanol; gradient: 40%–80% B 0–20 min, flow rate = 1.0 mL/min, T = 20°C; k′ = 4.8).

Biodistribution Studies

In vivo studies were performed with control and SRIF receptor-positive tumor-bearing rats. The experimental procedures used were approved officially and were in accordance with the guidelines on the use of living animals in scientific investigations. Male Lewis rats (250 ± 50 g) bearing an intrascapular exocrine pancreatic islet cell tumor were used for *in vivo* studies as described previously (19, 22).

Experiments were performed at 8 to 9 days after the inoculation of the tumor cells. At this time the tumors weighed 1–5 g. Prior to the application of the radiotracers, initial anesthesia was carried out by halothane or isoflurane followed by i.p. injection of hexobarbital (165 mg/kg). Subsequently, 100–200 μL of the radiolabeled octreotides were injected in the vena jugularis. The animals were sacrificed by cervical dislocation 5, 15, 30, 60, and 120 min after injection, and the organs of interest were rapidly dissected. The radioactivity was measured in weighted tissue samples using a γ-counter (Canberra-Packard, Frankfurt, Germany). Additional experiments were performed with normal NMRI mice to study the extent of hepatobiliary clearance of (2-[^{18}F]fluoropropionyl-(D)phe^1)-octreotide. Data are expessed in % injected dose/g tissue ± SEM (n = 3, unless otherwise stated). Table 1 summarizes the protocol used for the studies on the tumor-bearing rats.

In Vivo *Stability Studies*

The extent of *in vivo* degradation of the radiopharmaceuticals was analyzed by reversed-phase and size-exclusion chromatography. Urine samples were diluted 1:10 in HPLC solvent and directly analyzed using a reversed-phase column (see Quality Control section). Blood samples were immediately centrifuged at 4000 *g*. The plasma was subjected to size-exclusion chromatography (Sephadex G-25 column and BioSil SEC 250, 300 × 7.8 mm, BioRad, Richmond, VA) to determine protein-bound activity. Additionally, by adding a 1:1 mixture of MeOH/MeCN and second centrifugation, reversed-phase chromatography of the protein-free solution was performed to determine the amount of intact tracer. After homogenizing the tissue samples from liver, pancreas, kidneys, and tumor, similar analytical procedures were performed as described for the blood samples.

TABLE 3. Biodistribution Data of [^{67}Ga]-DFO-Octreotide in Male Lewis Rats Bearing an Exocrinic Pancreatic Islet Cell Tumor and Control Rats, 60 and 120 min postinjection (n = 3)

	Tumor-bearing rats		Control rats
Organ	60 min	120 min	60 min
Pituitary	0.58 ± 0.04	0.71 ± 0.06	—
Brain	0.01 ± 0.01	0.02 ± 0.01	—
Bone	0.26 ± 0.02	0.33 ± 0.15	—
Intestines	0.15 ± 0.02	0.13 ± 0.03	0.21 ± 0.05
Pancreas	0.59 ± 0.12	0.33 ± 0.02	—
Liver	0.81 ± 0.33	0.56 ± 0.21	0.26 ± 0.02
Blood	0.45 ± 0.07	0.58 ± 0.23	0.25 ± 0.05
Kidney	4.14 ± 0.36	2.71 ± 0.26	4.66 ± 0.95
Adrenals	3.35 ± 0.84	2.62 ± 0.35	—
Heart	0.23 ± 0.03	0.22 ± 0.11	0.08 ± 0.04
Tumor	0.82 ± 0.11	0.57 ± 0.18	—
Spleen	1.74 ± 0.89	0.76 ± 0.29	0.18 ± 0.04

TABLE 4. *Ex Vivo* Biodistribution Data of [^{86}Y]-DTPA-Octreotide in Male Lewis Rats Bearing an Exocrinic Pancreatic Islet Cell Tumor and Control Rats, 60 and 120 min postinjection (n = 3)

	Tumor-bearing rats		Control rats
Organ	60 min	120 min	60 min
Pituitary	0.63 ± 0.17	1.39 ± 1.17	2.03 ± 1.12
Brain	0.03 ± 0.01	0.02 ± 0.01	0.02 ± 0.01
Bone	1.31 ± 0.21	1.59 ± 0.14	0.23 ± 0.01
Intestines	0.17 ± 0.04	0.15 ± 0.07	0.08 ± 0.02
Pancreas	0.18 ± 0.02	0.15 ± 0.07	0.14 ± 0.01
Liver	0.65 ± 0.20	0.76 ± 0.01	0.24 ± 0.03
Blood	0.46 ± 0.05	0.13 ± 0.05	0.16 ± 0.01
Kidney	1.10 ± 0.07	0.98 ± 0.16	2.60 ± 0.18
Adrenals	0.25 ± 0.02	0.19 ± 0.04	0.79 ± 0.19
Heart	0.41 ± 0.02	0.27 ± 0.01	0.10 ± 0.01
Lung	0.50 ± 0.07	0.23 ± 0.05	0.16 ± 0.02
Tumor	0.44 ± 0.17	0.39 ± 0.05	—
Spleen	0.86 ± 0.58	0.95 ± 0.15	0.26 ± 0.02

Calculated data expressed as %injected dose/g (mean ± SD).

Pretreatment and Displacement Studies in Non-Tumor-Bearing Rats

For SRIF receptor-blocking studies, 1 mg/kg SMS 201-995 (octreotide) was administered i.v. into the vena jugularis as a 100-μL bolus 5 and 10 min prior to the injection of (2-[^{18}F]fluoro-propionyl-(D)phe^1)-octreotide. Alternatively, 1 mg/kg SMS 201-995 was administered subcutaneously 10 min prior to the injection of the radiotracer. For the displacement studies, 1.0 mg/kg SMS 201-995 were given i.v. 5, 10, and 20 min after injection of (2-[^{18}F]fluoropropionyl-(D)phe^1)-octreotide. All animals were sacrificed 60 min postinjection of the radiotracer. Subsequent determination of the activity accumulation in organs with high SRIF receptor density (adrenals, pancreas, and pituitary) (25, 34, 35) was performed as described above (biodistribution studies). Data are expressed as ratio of type (%ID/organ)/(%ID/organ control) ± SEM (n = 3, unless stated otherwise). The control animals (n = 3) were sacrificed after 60 min.

PET Data Acquisition and Imaging Studies

The PET measurements were performed with a PC-4096-15WB camera (SCANDITRONIX-GE, Uppsala, Sweden). The camera has an axial field of view of 10.5 cm; thus, the entire animal was positioned with its medial axis parallel to the middle plane of the scanner. Performance characteristics of the scanner have been previously described (38). For the purpose of attenuation correction, a transmission scan of 10 min was done before the tracer injection. The radiotracers were administered within 5 sec in a 100-μL volume. The injected activity was determined by measuring the injection syringe before and after application using a Curiemeter for fluorine-18 and a Ge(Li) detector for yttrium-86. Simultaneously with the tracer injection, dynamic PET scanning was started for 60, 75, or 120 min with intervals of 30 sec at the beginning and 10 min at the end. To optimize the sampling of the PET data, wobble and interleave mode was used. The interleave mode yields 30 image planes with an interplane distance of 3.2 mm. The reconstructed image resolution was about 5.5

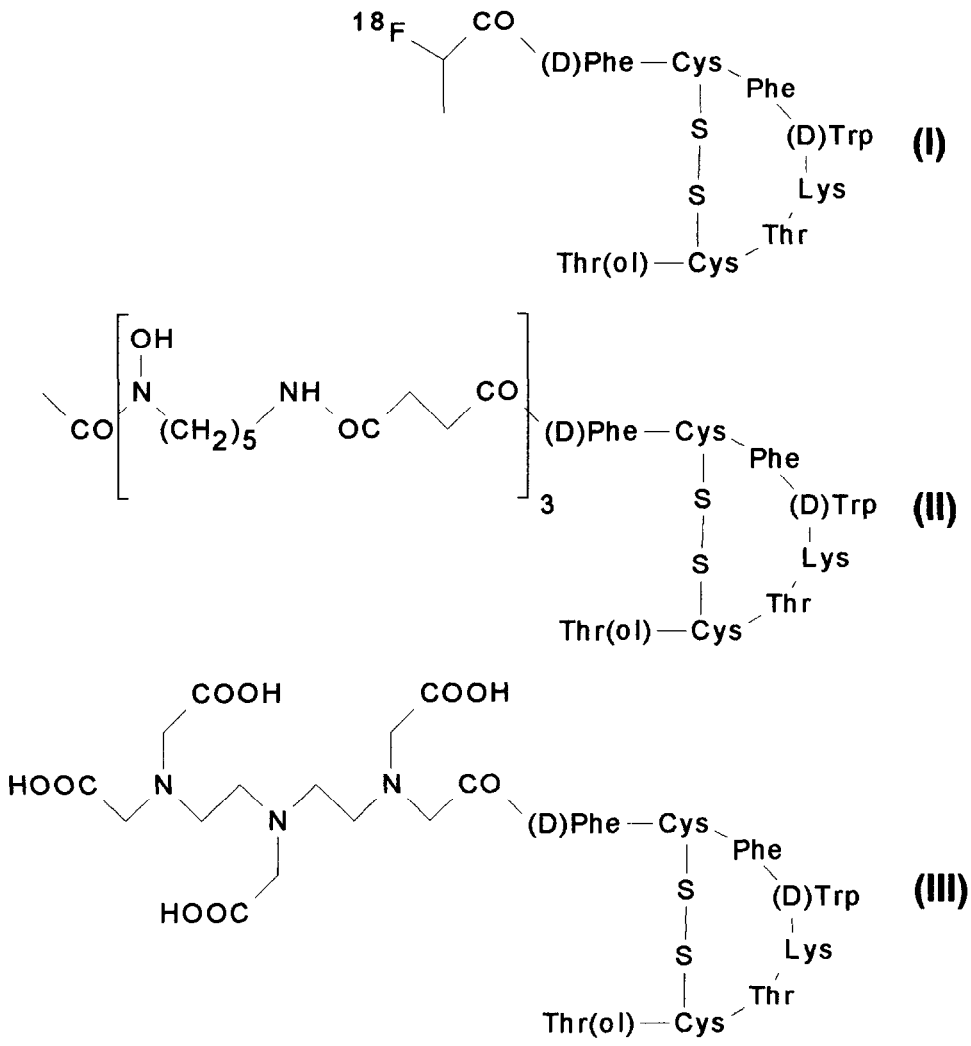

FIG. 1. Structures of the octreotide analogues 2-[^{18}F]fluoropropionyl-(D)phe^1-octreotide (I), DFO-(D)phe^1-octreotide (SDZ 216-927) (II), and DTPA-(D)phe^1-octreotide (SDZ 215-811) (III).

mm. The reconstructed PET images had a matrix size of 256 × 256 with a pixel size of 1 mm × 1 mm. For the definition of regions of interest (ROI) an image was used that summarizes the PET data from 10 min to 100 min. ROIs were placed over the liver, kidneys, bladder, and tumor. The reconstructed images were obtained in activity/volume (nCi/mL). Decay-corrected time-activity curves were calculated. No additional efforts were undertaken for the correction of partial-volume effects.

Additionally, absolute activity concentrations in the organs of interest were normalized to an injected activity of 1 μCi, thus providing information comparable to the data of the *ex vivo* biodistribution experiments in terms of %ID/g.

At the end of the PET measurements the animals were sacrificed and the organs of interest were measured in the same way as described in the *ex vivo* biodistribution experiments. Uptake kinetics measured by PET could thus be compared with biodistribution data at 60 and 120 min postinjection.

RESULTS

Radiopharmaceutical Syntheses

Synthesis of (2-[^{18}F]fluoropropionyl-(D)phe^1)-octreotide was accomplished within 120–130 min with radiochemical yields of 25% to 30% based on ^{18}F-fluoride. The specific activity of the HPLC-purified product was in the range of 38–42 GBq/μmoL peptide. Initial attempts to quantify the incorporation rates for both metal-labeled compounds by HPLC with commonly used C-18 matrices were unsuccessful because recovery of the injected yttrium-86 activity was not quantitative. Further experiments with an HPLC system consisted of fully peek-coated columns and capillaries showed quantitative recovery. The incorporation yield of gallium-67 into DFO-(D)phe^1-octreotide was generally >99.5% in 20 min. [^{67}Ga]-DFO-(D)phe^1-octreotide was obtained in a specific activity of 0.84 GBq/μmoL. The synthesis of [^{86}Y]-DTPA-(D)-phe^1-octreotide was quantitatively accomplished within 15 min and resulted in a specific activity of 17 GBq/μmoL.

Ex Vivo *Biodistribution*

The tissue distributions of radioactivity in the tumor-bearing rats 60 and 120 min after i.v. injection of the three tracers are shown in Tables 2–4.

Sixty min postinjection of (2-[^{18}F]fluoropropionyl-(D)phe^1)-octreotide most of the administered activity was found in the intestines, liver, pancreas, kidneys, and the tumor. However, the highest activity concentrations (% ID/g tissue) were located in adrenals, intestines, kidneys, and liver. The tumor and the organs with a high density of somatostatin receptors reached an activity concen-

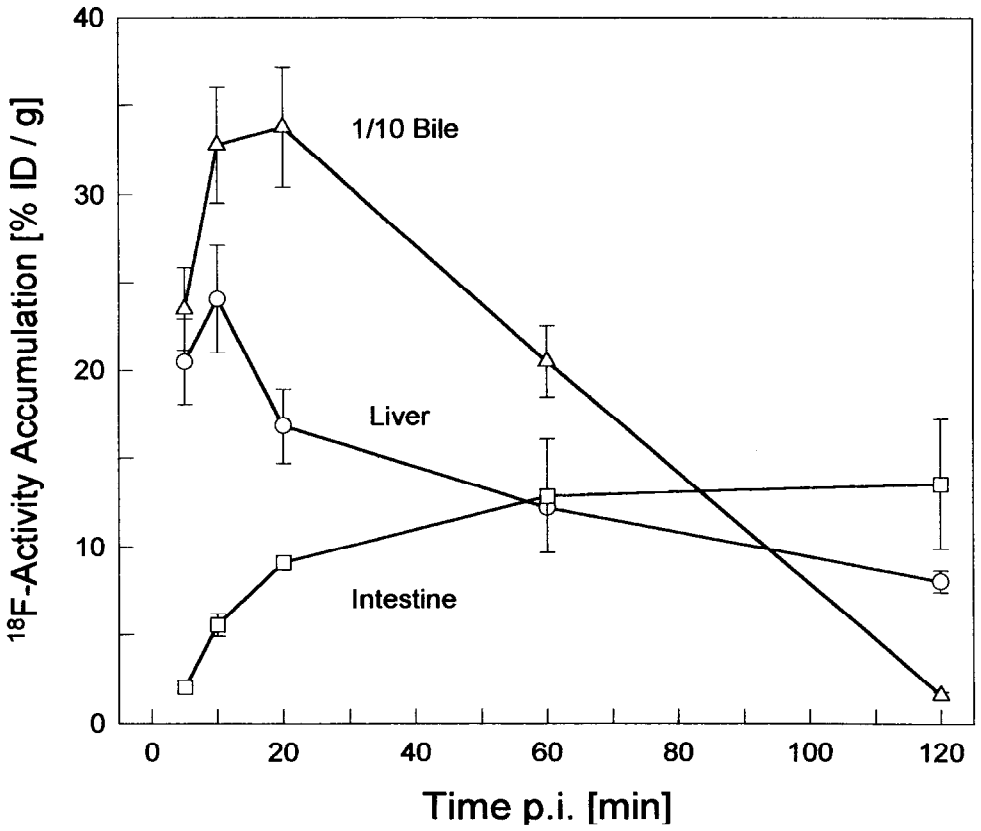

FIG. 2. Hepatobiliary clearance of (2-[^{18}F]fluoropropionyl-(D)phe^1)-octreotide. Uptake kinetics in liver, bile, and intestines of normal NMRI mice.

tration after 60 min of 0.5% ID/g (tumor), 2.4% ID/g (adrenals), 0.7% ID/g (pancreas), and 0.7% ID/g (pituitary gland), respectively. There was a significant release of radioligand from the organs of interest. Between 1 h and 2 h postinjection, ^{18}F-activity concentration in the tumor decreased from 0.52 ± 0.24 to 0.17 ± 0.04% ID/g. The blood clearance was also rapid, and led to values of 0.1% ID/g after 60 min and 0.04% ID/g after 120 min.

As the ^{18}F-activity located in the kidneys decreased, activity continuously increased in the intestines, from 0.2% ID/g 5 min postinjection to 1.9% ID/g after 60 min, a total of about 40% of the administered activity. As depicted in Figure 2, additional experiments with NMRI mice revealed that (2-[^{18}F]fluoropropionyl-(D)phe^1)-octreotide exhibited a fast liver uptake, achieving a maximum at about 10 min. This uptake paralleled the high accumulation of the activity in the bile and resulted in a continuous increase of the activity concentration in the intestine.

For [^{67}Ga]-DFO-(D)phe^1-octreotide, the highest activity concentrations 60 min postinjection were detected in kidneys, adrenals, and spleen. Whereas the accumulation in tumor, pituitary, and pancreas was found to be similar for all three organs (0.8, 0.6, and 0.6% ID/g), the adrenals reached 3.35% ID/g. The tracer was mainly cleared from the circulation by renal excretion. Thus, [^{67}Ga]-activity located in the liver did not exceed 0.8% after 1 h. Furthermore, about 2% of the administered dose was found in the intestines, which corresponded to 0.13% ID/g at 120 min postinjection. The tumor showed higher activity concentrations, 0.82 ± 0.11 and 0.57 ± 0.18% ID/g after 1 and 2 h, respectively.

Sixty minutes postinjection of ([^{86}Y]-DTPA-(D)phe^1)-octreotide high uptake of radioactivity was measured in the bone, kidneys, spleen, and liver of the animals. High yttrium-86 uptake was also exhibited by the pituitary (0.6% ID/g, 60 min; 1.4% ID/g, 120 min) and to a lower extent by the adrenals and pancreas. Accumulation of radioactivity was 0.44 ± 0.17 and 0.39 ± 0.05% ID/g at the tumor site 60 and 120 min postinjection. The [^{86}Y]-DTPA-(D)phe^1-octreotide was cleared from the circulation mainly by the kidneys but also by the liver.

SRIF Receptor Blocking and Displacement Studies

Results of the blocking and displacement studies in NMRI mice are shown in Figure 3. Blocking with 1 mg/kg SDZ 201-995 5 min prior to the injection of the (2-[^{18}F]fluoropropionyl-(D)phe^1)-octreotide reduced the activity concentration in the adrenals to about 14% of control. A similar effect was observed when SMS 201-995 was

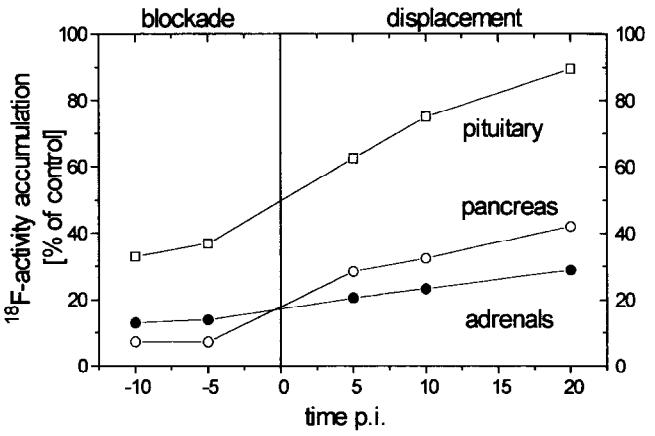

FIG. 3. Pretreatment and displacement studies on non-tumor-bearing male Lewis rats.

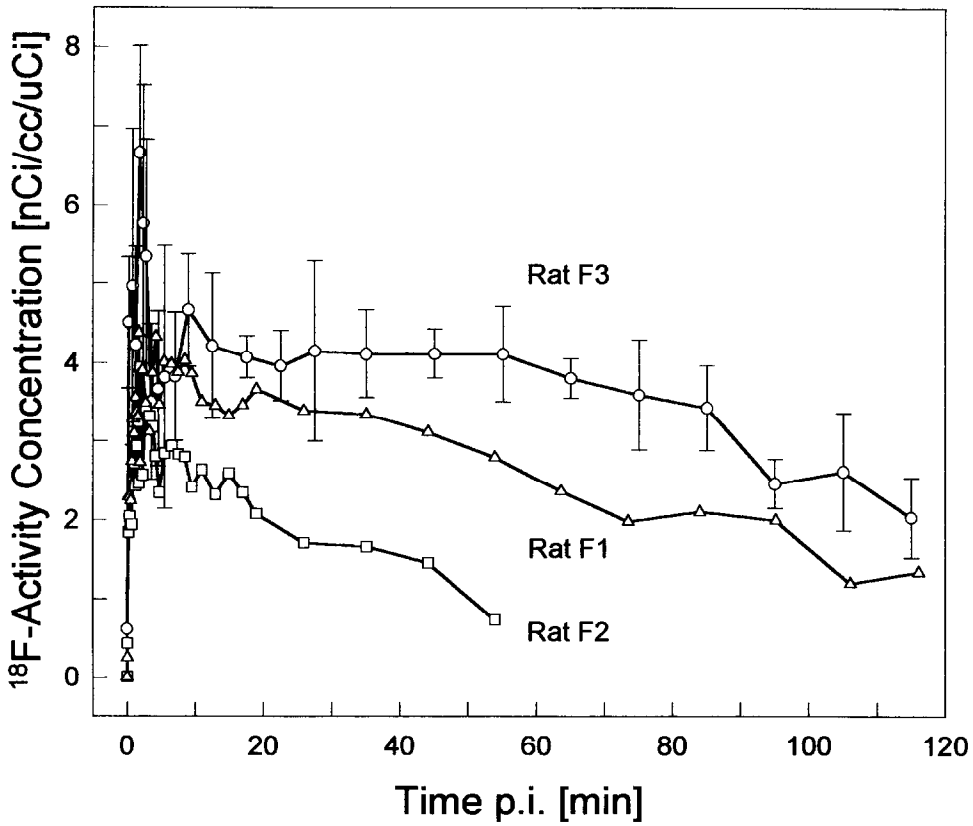

FIG. 4. Tumor uptake kinetics of (2-[^{18}F]fluoropropionyl-(D)phe^1)-octreotide in three male Lewis rats bearing an exocrine pancreatic islet cell tumor as measured by PET.

administered subcutaneously (data not shown). Receptor blocking was also achieved in the pancreas, leading to reduced accumulation of the radiotracer to about 7% of control. However, the blocking was not as efficient for the pituitary gland (37% of control, 5 min prior to injection).

Similar trends were observed in the displacement studies. Administration of 1 mg/kg SDZ 201-995 at 10 min postinjection displaced about 77% of the ^{18}F-activity in the adrenals, 68% in the pancreas, but only about 25% in the pituitary gland.

In Vivo *Stability Studies*

Blood and urine specimens as well as tumor, liver, and kidney homogenates were subjected to HPLC and size-exclusion chromatography analysis. Even for the longest observation time (120 min) only intact (2-[^{18}F]fluoropropionyl-(D)phe^1)-octreotide (>98%) was found in all specimens. Protein-bound activity, determined by protein precipitation of blood samples, was less than 2%.

Only about 10% of intact [^{67}Ga]-DFO-(D)phe^1-octreotide was found in blood 15 min postinjection, as determined by protein precipitation with 1:1 MeOH/MeCN followed by reversed-phase chromatography analysis of the supernatant solution. After 120 min, no tracer was left. The same trend was observed in the liver samples, whereas the activity found in kidney and tumor represented higher proportions of intact tracer.

Urine samples taken 60 min after the administration of ^{86}Y-labeled octreotide showed that about 60% of the radiometal was still complexed by DTPA-octreotide, while the amount of intact tracer in the blood was less than 10%.

PET Studies

Results of the PET measurements are summarized in Figures 4–7. Figure 4 illustrates the individual tumor uptake kinetics of (2-[^{18}F]fluoropropionyl-(D)phe^1)-octreotide in three individual rats. The data are normalized to 1 μCi injected activity. Results of the three PET experiments showed a remarkable uniformity of the maximum accumulation of (2-[^{18}F]fluoropropionyl-(D)phe^1)-octreotide as well as of the uptake kinetics.

After injection of (2-[^{18}F]fluoropropionyl-(D)phe^1)-octreotide the tumor was visible in less than 1 min. Thereafter, the activity concentration increased slightly up to about 3 min. The maximum ^{18}F-activity concentration localized in the tumor of different animals varied from 2.5 to 4.8 (nCi/cc)/μCi, which corresponded to an average value of 0.4 ± 0.1% ID/g at 2.5 min postinjection. The release of (2-[^{18}F]fluoro-propionyl-(D)phe^1)-octreotide had a $k_{off} = 10 \pm 2 \cdot 10^{-5}$ s^{-1}. Figure 5 compares the uptake kinetics of (2-[^{18}F]fluoropropionyl-(D)phe^1)-octreotide in the tumor with that in the liver, kidneys, and bladder of rat F3. Activity in the kidneys peaked at about 15 min postinjection with maximum ^{18}F-activity concentrations being one order of magnitude higher than that of the tumor.

Transfer of the tracer to the bladder led to a fast and continuous decrease of ^{18}F-activity concentration in the kidneys. About 20 min after injection, the bladder had become the organ of highest activity concentration and was visible as a hot spot in the PET images. Owing to the slower excretion rate, the liver reached maximum activity concentrations at about 30 min postinjection. Up to 2 h postinjection the ^{18}F-activity concentration remained almost constant in that organ.

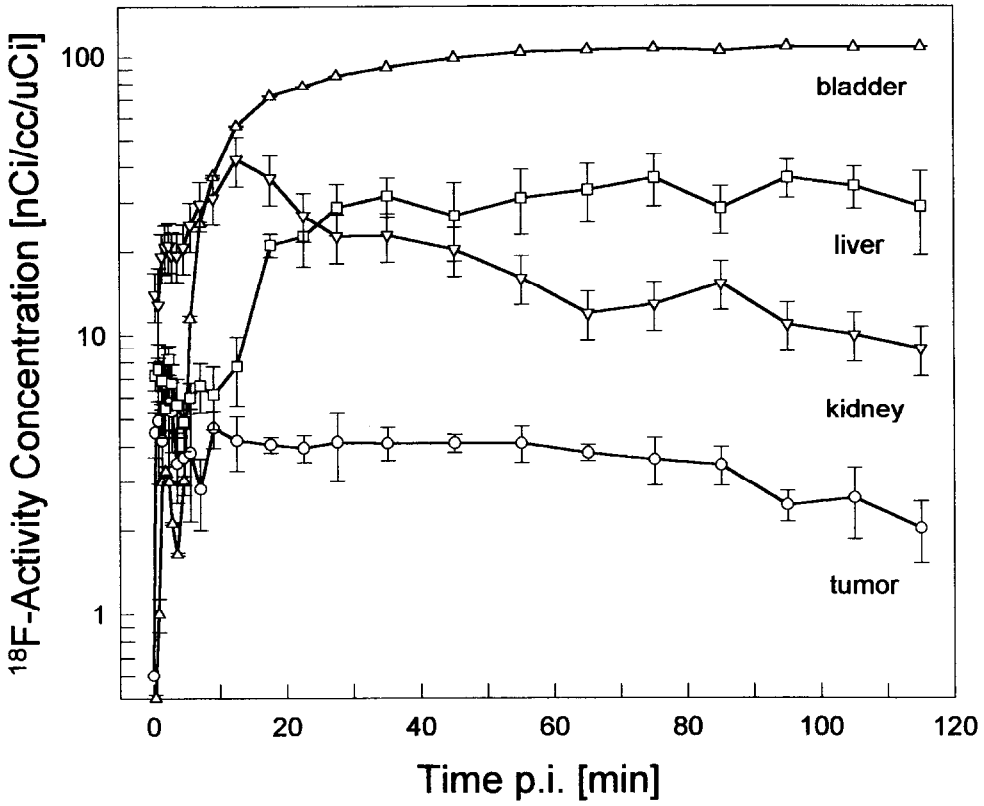

FIG. 5. Uptake kinetics of (2-[^{18}F]fluoropropionyl-(D)phe^1)-octreotide in the tumor, liver, bladder, and kidney of a male Lewis rat bearing an exocrine pancreatic islet cell tumor as simultaneously measured by PET.

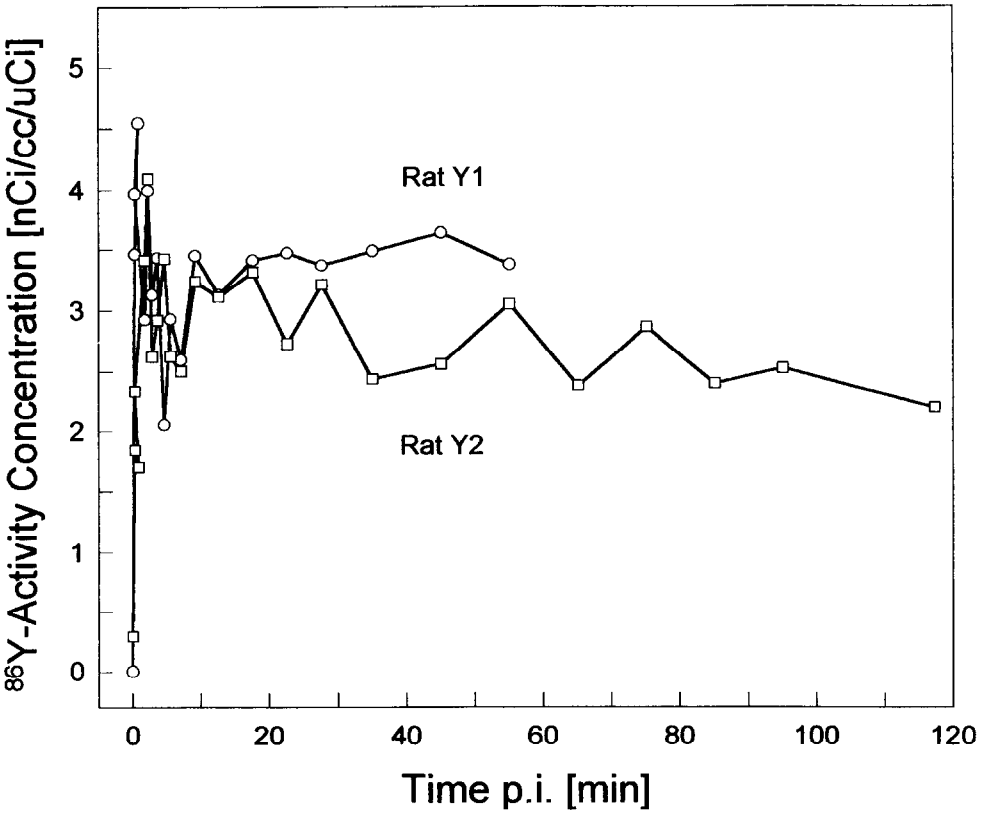

FIG. 6. Tumor uptake kinetics of ([^{86}Y]-DTPA-(D)phe^1)-octreotide of two rats bearing an exocrine pancreatic islet cell tumor as measured by PET.

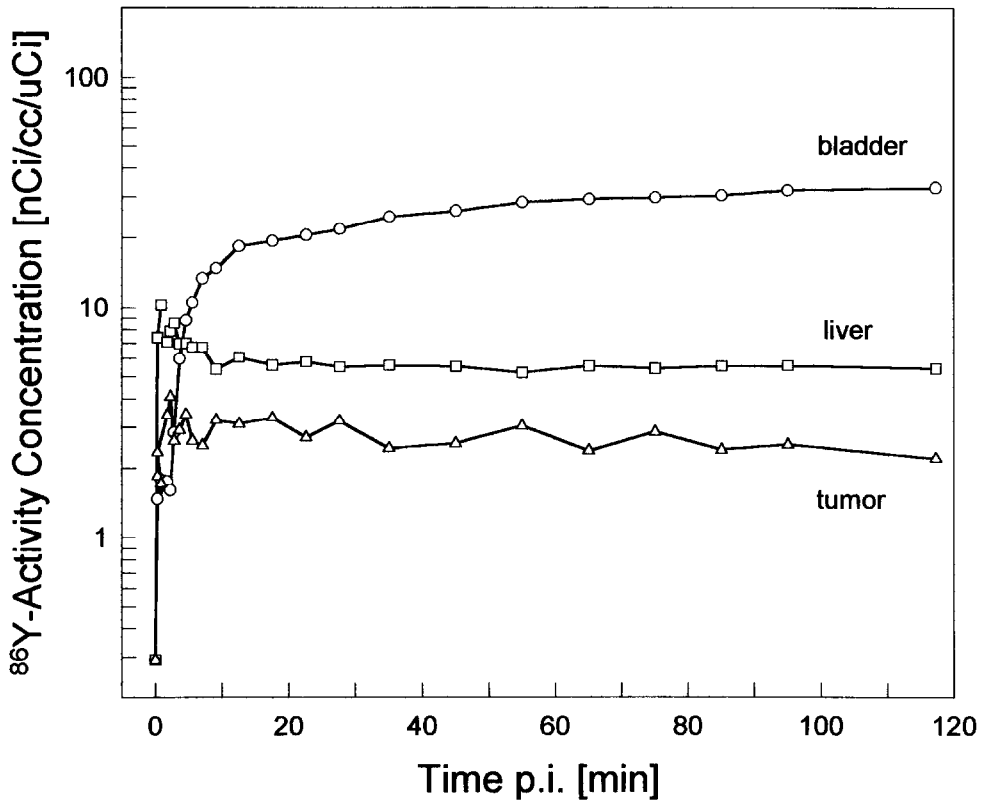

FIG. 7. Uptake kinetics of ([^{86}Y]-DTPA-(D)phe^1)-octreotide in the tumor, liver and bladder of a male Lewis rat bearing an exocrine pancreatic islet cell tumor as simultaneously measured by PET.

Figure 6 depicts the accumulation kinetics of ([^{86}Y]-DTPA-(D)phe^1)-octreotide in the tumors of two different rats. Both the maximum ^{86}Y-activity concentration (3.5 ± 0.5 nCi/cc/μCi injected) and their uptake kinetics (maximum accumulation at 3.5 ± 0.5 min postinjection) were similar. The maxima were followed by a small and continuous release, with a $k_{off} = 3.1 \pm 1.3 \cdot 10^{-5}\ s^{-1}$. Figure 7 compares the tumor-uptake kinetics with those for liver and bladder, measured simultaneously in rat Y1.

DISCUSSION

The aim of the present study was to evaluate three differently labeled octreotide derivatives—((2-[^{18}F]fluoropropionyl-(D)phe^1)-octreotide, ([^{67}Ga]-DFO-B-succinyl-(D)phe^1)-octreotide, and ([^{86}Y]-DTPA-(D)phe^1)-octreotide)—for *in vivo* tumor diagnosis with PET by characterizing their quantitative uptake and binding kinetics and the extent of *in vivo* degradation in rats bearing an exocrine pancreatic tumor.

TABLE 5. Displacement of [^{125}I]-Tyr^3-Octreotide by Various SRIF Analogues (Determined on Rat Cortex Membranes)

SRIF-Analogue	Displacement of [^{125}I]-Tyr^3-octreotide (pK_i values)
SRIF-14	9.55 ± 0.15 (11)
octreotide	9.33 ± 0.06 (11)
([^{nat}In]-DTPA-(D)phe^1)-octreotide	8.70 ± 0.20 (4)
([^{nat}Ga]-DFO-(D)phe^1)-octreotide	9.6 (42)
(2-[^{18}F]fluoropropionyl-(D)phe^1)-octreotide	8.60 ± 0.20 (17)

The pK_i values of the compounds of interest are listed in Table 5. The values of fluorine- and gallium-labeled octreotide are within the same order of magnitude. It is assumed that substitution of indium-111 for yttrium-86 in [^{111}In]-DTPA-(D)phe^1)-octreotide does not significantly affect its pK_i. Thus, the suitability of these compounds for *in vivo* imaging of tumors that express the somatostatin receptor is determined mainly by the radionuclide and the corresponding coupling chemistry, which in turn modifies the specific tracer biodistribution, the metabolic behavior, and the stability *in vivo*.

The lipophilicity of fluorine-18-labeled octreotide accounts for why its biodistribution differs from those of the other tracers. The fast liver uptake of (2-[^{18}F]fluoropropionyl-(D)phe^1)-octreotide is followed by an increasing activity concentration in the intestines over time (Table 2). The hepatobiliary excretion of (2-[^{18}F]fluoropropionyl-(D)phe^1)-octreotide is in accordance with literature data available for [^{125}I]Tyr^3-octreotide (5, 21), [^{3}H]octreotide (26), [^{14}C]octreotide (26), and unlabeled octreotide (15) as well as data observed in this study with NMRI mice (Fig. 2). However, the extent of clearance via this pathway seems to be significantly higher for the iodinated compound.

De Jong *et al.* (21) reported that in a perfused rat liver test system more than 60% of [^{125}I]-Tyr^3-octreotide was cleared into the bile within 1 h. Bakker *et al.* (5) found a cumulative ^{123}I-activity of 62% of the injected dose 30 min after i.v. administration of the tracer in the liver (12 ± 2% ID) and intestines (50 ± 10% ID) of rats. In contrast, 1 h postinjection of ^{18}F-octreotide only about 45% of the administered dose was located in these organs (liver 11 ± 1% ID; intestines 34 ± 5% ID).

Like ([^{111}In]-DTPA-(D)phe^1)-octreotide (6, 23), [^{67}Ga]-DFO-octreotide and ([^{86}Y]-DTPA-(D)phe^1)-octreotide were mainly excreted via the kidneys. Except for the very lipophilic [^{99m}Tc]-PnAO-octreotide (27), ^{86}Y-DTPA-octreotide exhibits the highest

TABLE 6. Hepatobiliary Excretion of Different Radiolabeled Octreotide Derivatives: Kidney to Liver and Kidney to Intestines Ratios

Organ Ratio	[^{111}In]-DTPA-octr. (1 h postinjection)	[^{67}Ga]-DFO-octr. (1 h postinjection)	[^{86}Y]-DTPA-octr. (1 h postinjection)	2-[^{18}F]-Fluoroprop. octr. (1 h postinjection)	[^{123}I]Tyr^3-octr. (0.5 h postinjection)	[^{99m}Tc]-PnAO-octr. (1.5 h postinjection)
Kidney/Liver	6.38 (11)	5.11	1.69	1.06	1.15 (5)	0.34 (27)
Kidney/Intestine	15.16 (11)	27.60	6.47	0.68	0.56 (5)	1.05 (27)

hepatobiliary uptake among the metal ion-labeled octreotide analogues. This is demonstrated by the kidney-to-liver and kidney-to-intestine ratio, which are significantly lower for the ^{86}Y-labeled octreotide (Table 6). Whether this is due to the kind of complex or to metal ion uptake remains to be determined. However, the desirable fast renal excretion of the radiometal-labeled octreotide derivatives, which minimizes diffuse activity distribution in the abdominal region, is offset by the gallium-67/68, indium-111, and yttrium-86 activity remaining in the kidneys (6, 11, 23, 42). This leads to high kidney-to-tumor ratios even at long observation times. Whether this phenomenon reflects transcomplexation or tubular reabsorption of the peptide complex after glomerular filtration (6, 23) is unclear. In this context the effect of lysine on the uptake of peptides and monoclonal antibodies in the kidneys is of interest (8).

The highest tumor-to-tissue ratios were obtained with ([^{67}Ga]-DFO-B-succinyl-(D)phe^1)-octreotide (Table 8). With the exception of the kidneys (high renal clearance), the tumor-to-tissue ratios for kidney, liver, intestines, and bone are larger than unity. In the case of (2-[^{18}F]fluoropropionyl-(D)phe^1)-octreotide, however, all the organs except the bones show tumor-to-organ ratios < 1. The low tumor-to-tissue ratios obtained for ([^{86}Y]-DTPA-(D)phe^1)-octreotide (Table 8) reflect the instability of the yttrium-DTPA-complex, tumor-to-bone ratio < 1, as well as the clearance via both renal and hepatobiliary pathways, as reflected by tumor-to-kidney and tumor-to-liver ratios < 1.

^{18}F-Octreotide showed the fastest blood clearance, resulting in tumor-to-blood ratios of 5.2 at 1 h and 4.2 at 2 h. The blood clearance of ^{67}Ga-octreotide was slower than that of ^{18}F-octreotide and similar to [^{86}Y]-DTPA-octreotide. Thus, despite a somewhat higher tumor uptake of ^{67}Ga-octreotide, the tumor-to-blood ratios after 1 h are lower for both metal-labeled compounds when compared to ^{18}F-octreotide (see Figure 8).

In vivo stability studies were performed to quantitate the amount of intact tracers in samples of blood, urine, tumor, kidney, and liver. The experiments showed exclusively intact (2-[^{18}F]fluoropropionyl-(D)phe^1)-octreotide during the entire 120 min of observation. That result demonstrates the metabolic stability of the amide bond formed during ^{18}F-labeling. The low ^{18}F-activity accumulation in bone after 2 h indicates high *in vivo* stability against defluorination and again shows that prosthetic groups containing aliphatic fluorine-18 do not generally undergo extensive *in vivo* defluorination (32). Thus, in the case of octreotide, ^{18}F-fluorination by aromatic moieties such as esters of 4-fluorobenzoic acid (16, 46, 47) is unnecessary. Moreover, the use of 4-[^{18}F]fluorobenzoic acid as a prosthetic group for octreotide labeling would further increase hepatobiliary clearance.

The stability of the ^{67}Ga-labeled compound differed from that of ^{18}F-octreotide. The activity located in the tumor and extracted from kidneys indicates a low degradation of the tracer or release of the radiometal in these compartments. However, an increased degradation was detected in liver and blood. The rapid release of the radiometal from [^{86}Y]-DTPA-(D)phe^1-octreotide (<10% intact [^{86}Y]-DTPA-(D)phe^1-octreotide in blood samples after 60 min) was evident and also manifested by a bone accumulation of 1.3 (1 h postinjection) and 1.5 (2 h postinjection) %ID/g, respectively. However, because of the fast renal excretion, about 60% of the activity in the urine was still intact after 60 min.

These data reveal the limited usefulness of unmodified DTPA as a chelating moiety for *in vivo* studies using radioyttrium, wherein the linkage to octreotide is performed by the coupling of phe^1 to a carboxylic group of DTPA. However, liberation of the radiometal might be overcome by using modified linker-chelator units such as ethylene glycol bis(succinimidyl succinate-(1-(*p*-amino-benzyl)-DTPA)) (EGS-ABDTPA), *di*-succinimidyl tartrate-ABDTPA (DST-ABDTPA), *di*-succinimidyl suberate-ABDTPA (DSS-ABDTPA),

TABLE 7. Tumor Uptake Kinetics and Residence Time of (2-[^{18}F]fluoropropionyl-(D)phe^1)-Octreotide [I], [^{67}Ga]-DFO-(D)phe^1-Octreotide [II] and [^{86}Y]-DTPA-(D)phe^1-Octreotide [III] in Tumor-Bearing Rats as Derived from PET Measures and *Ex Vivo* Biodistribution Data

Compound	Time postinjection (min)	Tumor uptake: PET (%iD/ml)	Tumor uptake: *Ex vivo* biodistribution (%iD/g)	k_{off} ($\cdot 10^{-5}$ s^{-1})
[I]	5	0.39 ± 0.17	0.43 ± 0.28	
	60	0.40 ± 0.05	0.52 ± 0.24	10 ± 2
	120	0.20 ± 0.05	0.17 ± 0.04	
[II]	5		0.34 ± 0.03	
	60		0.82 ± 0.11	3.0 ± 0.5
	120		0.57 ± 0.18	
[III]	60	0.31 ± 0.05	0.44 ± 0.17	3.1 ± 1.3
	120	0.26 ± 0.01	0.39 ± 0.05	

TABLE 8. Tumor-to-Organ Ratios of (2-[^{18}F]fluoropropionyl-(D)phe^1)-Octreotide [I], [^{67}Ga]-DFO-(D)phe^1-Octreotide [II[and ([^{86}Y]-DTPA-(D)phe^1)-Octreotide [III] in Tumor-Bearing Rats as Derived from *Ex Vivo* Biodistribution Data (60 and 120 min postinjection, n = 3)

Compound	Tumor to intestines	Tumor to kidneys	Tumor to liver	Tumor to bone
[I]				
60 min	0.28 ± 0.09	0.40 ± 0.11	0.42 ± 0.19	12.5 ± 2.5
120 min	0.09 ± 0.01	0.27 ± 0.01	0.20 ± 0.08	3.72 ± 0.69
[II]				
60 min	5.64 ± 0.69	0.20 ± 0.02	1.09 ± 0.18	3.13 ± 0.35
120 min	4.29 ± 0.39	0.21 ± 0.05	1.05 ± 0.14	2.14 ± 0.20
[III]				
60 min	1.93 ± 0.23	0.31 ± 0.05	0.53 ± 0.18	0.23 ± 0.01
120 min	3.90 ± 1.19	0.42 ± 0.02	0.54 ± 0.05	0.25 ± 0.01

1-(*p*-isothiocyanatobenzyl)-DTPA (ITCB-DTPA) (33), or other chelators such as DOTA (12, 28).

Dynamic PET measurements of biodistribution showed a good correlation with the *ex vivo* biodistribution; the maximum difference was about 25% (Table 7). These measurements yielded three parameters for (2-[^{18}F]fluoropropionyl-(D)phe^1)-octreotide and ([^{86}Y]-DTPA-(D)phe^1)-octreotide: (a) the time to reach the maximum tumor uptake; (b) the maximum tumor uptake in terms of %ID/g, and (c) k_{off} values for the release of activity from the tumors.

For both radiolabeled octreotide derivatives the tumor uptake was rapid. Maximum accumulation was achieved at 2 ± 1 min and 3.5 ± 0.5 min after injection of (2-[^{18}F]fluoropropionyl-(D)phe^1)-octreotide and ([^{86}Y]-DTPA-(D)phe^1)-octreotide, respectively, substantially faster than the 15 min in the case of ([^{68}Ga]-DFO-B-succinyl-(D)phe^1)-octreotide (42). According to the PET measurements, the maximum tumor uptake was 0.4 ± 0.1% ID/g, 0.35 ± 0.05% ID/g, and 0.9% ID/g for ^{18}F-, ^{86}Y- and ^{68}Ga-labeled octreotide, respectively.

The ^{18}F-activity uptake in the tumor as measured *ex vivo* 60 min postinjection showed values of 0.24, 0.65, and 0.66% ID/g (0.52 ± 0.24). Data obtained from quantitative PET scans for animals F1, F2, and F3 showed values of 0.4 ± 0.1% ID/g at 2 h postinjection, which were consistent with the *ex vivo* distribution data obtained for the same animals directly after the PET scans.

Differences in endogenous somatostatin levels might account for the within-group and between-group variability (20, 22, 39, 40). Accordingly, only the kinetic data were used to compare the three different tracers.

Finally, the release of activity from the tumor was quantified. Release of (2-[^{18}F]fluoropropionyl-(D)phe^1)-octreotide from the tumor appeared to be faster than that of [^{68}Ga]-DFO-(D)phe^1-octreotide and [^{86}Y]-DTPA-(D)phe^1-octreotide, with k_{off} rates of $10 \pm 2 \cdot 10^{-5}$ s^{-1}, $3.0 \pm 0.5 \cdot 10^{-5}$ s^{-1} (42), and $3.1 \pm 1.3 \cdot 10^{-5}$ s^{-1}, respectively. Whether the slower release of activity from the tumor when using metal chelate octreotide analogues might be caused by internalization phenomena (2, 13, 14, 29–31) requires further investigations. The unspecific partitioning of (2-[^{18}F]fluoropropionyl-(D)phe^1)-octreotide into membranes (41), caused by the higher lipophilicity of this octreotide derivative, is another possibility that warrants investigation.

The blocking and displacement of (2-[^{18}F]fluoropropionyl-(D)phe^1)-octreotide bound to the SRIF receptor revealed some differences with respect to the organs investigated. Compared to the pituitary gland, receptor blocking was more successful for the adrenals and the pancreas. Using [^{123}I]-RC-160, Breeman *et al.* (9)

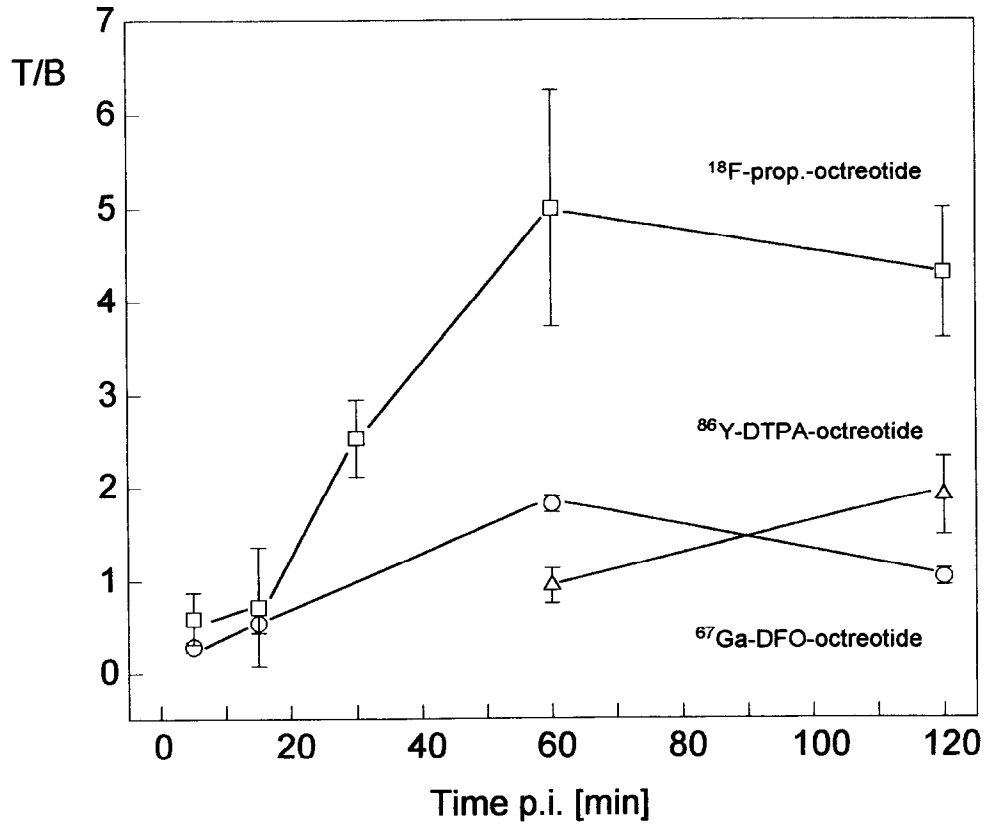

FIG. 8. Tumor-to-blood ratios for (2-[^{18}F]fluoropropionyl-(D)phe^1)-octreotide and ([^{67}Ga]-DFO-(D)-phe^1)-octreotide as measured by *ex vivo* biodistribution.

found a reduction in ^{123}I-activity in the pancreas, adrenals, and pituitary of non-tumor-bearing rats to about 12%, 22%, and 12% of control and 2%, 10%, and 2% of control using [^{123}I]-Tyr^3-octreotide (in both cases measured at 4 h postinjection; pretreatment with 1 mg RC-160 and 1 mg I-Tyr^3-octreotide, respectively, 45 min prior to the injection of the radiotracer). Displacement of the ^{18}F-activity was also more successful with respect to pancreas and adrenals compared to the pituitary gland. The lower displacement rate 10 and 20 min postinjection of the radiotracer may be a result of receptor-ligand endocytosis such as that observed for somatostatin-24 and somatostatin-14 (13, 14, 29).

CONCLUSION

The major advantages of ^{18}F-labeled octreotide when compared to ^{68}Ga-labeled octreotide can be attributed to the fast blood clearance and the high *in vivo* stability of the fluorinated compound. The advantage of ^{68}Ga-labeled octreotide is the ease of synthesis and the commercially available ^{68}Ga-generators. Owing to the hepatobiliary excretion of (2-[^{18}F]fluoropropionyl-(D)phe^1)-octreotide, the interpretation of images of abdominal-located tumors may be complicated, as noted in previously described SPET studies using [^{123}I]Tyr^3-octreotide. However, with the development of less lipophilic somatostatin derivatives, such as the glycated SDZ CO 611 (1, 15), which exhibits predominantly renal excretion, ^{18}F-labeling of these analogues may lead to more suitable PET tracers for quantitative mapping of somatostatin receptors.

Further *in vitro* and *in vivo* investigations with potential PET and SPET tracers using SSTR-1 to SSTR-5 subtype-specific somatostatin analogues should lead to a better understanding of tracer-specific tissue accumulation and thus may allow more accurate tumor targeting with synthetic somatostatin receptor ligands. Because of the low steric impairment and the closest structure of (2-[^{18}F]fluoropropionyl-(D)phe^1)-octreotide to SMS 201-995, the ^{18}F-labeled analogue may be the most suitable candidate for such studies.

In view of combining diagnosis, dosimetric calculation, and endoradiotherapy, the use of both yttrium-86 and yttrium-90 for labeling of octreotide precursors linked to suitable chelator moities may support an improved radiochemical design of better radiotherapeutics. However, owing to the instability of yttrium-labeled DTPA-(D)phe^1-octreotide, more stable chelator structures are mandatory. An improvement was already made by using a bifunctional DTPA, yielding an *in vivo* more stable octadentate DTPA-octreotide analogue (45).

Finally, the factors that determine the accumulation of the different tracers in SSTR receptor-positive tissues remain unclear. In particular, the role of endocytosis and internalization of the intact radiolabeled octreotides or mechanisms that trap radiometals requires further investigation.

The authors would like to thank the teams of the JSW BC 1710 and CV-28 cyclotrons for radioisotope production and Fr. Theelen for assistance in the PET measurements.

References

1. Albert R., Marbach P., Bauer P., Briner U., Fricker G., Bruns C. *et al.* (1993) SDZ CO 611: A highly potent glycated analog of somatostatin with improved oral activity. *Life Sci.* **53,** 517–525.
2. Amherdt M., Patel Y. C. and Orci L. (1989) Binding and internalization of somatostatin, insulin and glucagon by cultured rat islet cells. *J. Clin. Inverst.* **84,** 412–417.
3. Anderson C. J., Pajeau T. S., Edwards W. B., Sherman E. L. C., Rogers B. E. and Welch M. J. (1995) In vitro and in vivo evaluation of copper-64-octreotide conjugates. *J. Nucl. Med.* **36,** 2315–2325.
4. Bakker W. H., Albert A., Bruns C., Breeman W. A. P., Hofland L. J., Marbach P. *et al.* (1991) [^{111}In-DTPA-D-phe^1]-Octreotide, a potential radiopharmaceutical for imaging of somatostatin receptor-positive tumors: Synthesis, radiolabeling and in vitro validation. *Life Sci.* **49,** 1583–1591.
5. Bakker W. H., Krenning E. P., Breeman W. H., Koper J. W., Kooij P. P., Reubi J. C. *et al.* (1990) Receptor scintigraphy with radioiodinated somatostatin analogue: Radiolabeling, purification, biologic activity and in vivo application in animals. *J. Nucl. Med.* **31,** 1501–1509.
6. Bakker W. H., Krenning E. P., Reubi J. C., Breeman W. A. P., Setyono-Han B., de Jong M. *et al.* (1991) In vivo application of [^{111}In-DTPA-Dphe^1]-octreotide for detection of somatostatin receptor-positive tumors in rats. *Life Sci.* **49**(22), 1593–1601.
7. Banks W., Schally A. V., Barrera C. M., Fasold M. B., Durham D. A., Csernus V. J. *et al.* (1990) Permeability of the murine blood-brain barrier to some octapeptide analogs of somatostatin. *Proc. Natl. Acad. Sci. USA.* **87,** 6762–6766.
8. Behr T. M., Sharkey R. M., Juweit M., Aninipot R., Griffiths G. L. and Goldenberg D. M. (1995) Reduction of kidney uptake of radiolabeled monoclonal antibody (Mab) fragments: Preclinical and initial clinical results. 42nd Annual Meeting of the Society of Nuclear Medicine, *J. Nucl. Med.* **36,** 19P.
9. Breeman W. A. P., Hofland L. J., Bakker M., van der Pluijm M., van Koetsveld P. M., de Jong M. *et al.* (1993) Radioiodinated somatostatin analogue RC-160: Preparation, biological activity, in vivo application in rats and comparison with [^{123}I-Tyr^3]octreotide. *Eur. J. Nucl. Med.* **20,** 1089–1094.
10. Breeman W. A. P., Hofland L. J., van der Pluijm M., van Koetsveld P. M., de Jong M., Seytono-Han B. *et al.* (1994) A new radiolabelled somatostatin analogue [^{111}In-DTPA-D-Phe^1]RC-160: Preparation, biological activity, receptor scintigraphy in rats and comparison with [^{111}In-DTPA-D-Phe^1]octreotide. *Eur. J. Nucl. Med.* **21,** 328.
11. Bruns C., Stolz B., Albert R., Marbach P. and Pless J. (1993) OctreoScan®111 for Imaging of a somatostatin receptor-positive islet cell tumor in rat. *Horm. Metab. Res. Suppl.* Ser. **27,** 4–11.
12. Desreux J. F. (1980) Nuclear magnetic resonance spectroscopy of lanthanide complexes with a tetraacetic tetraaza macrocycle: Unusual conformation properties. *Inorg. Chem.* **19,** 1319–1324.
13. Draznin B., Mehler P. S., Leitner J. W., Sussman K. E., Dahl R., Vatter R. *et al.* (1985) Localization of somatostatin receptors secretion vesicles in anterior pituitary cells and pancreatic islets. *J. Receptor Res.* **5,** 83.
14. Draznin B., Sherman N., Sussman K. E., Dahl R. and Vatter R. (1985) Internalization and cellular processing of somatostatin in primary culture of rat anterior pituitary cells. *Endocrinology* **117,** 960.
15. Fricker G., Dubost V., Schwab D., Bruns C. and Thiele C. (1994) Heterogeneity in hepatic transport of somatostatin analog octapeptides. *Hepatology* **20,** 191–200.
16. Guhlke S., Coenen H. H. and Stöcklin G. (1994) Fluoroacylation agents based on small n.c.a [^{18}F]fluorocarboxylic acids. *Appl. Radiat. Isot.* **45,** 715.
17. Guhlke S., Wester H. J., Bruns C. and Stöcklin G. (1994) (2-[^{18}F]Fluoropropionyl-(D)phe^1)-octreotide, a potential radiopharmaceutical for quantitative somatostatin receptor imaging with PET: Synthesis, radiolabeling, *in vitro* validation and biodistribution in mice. *Nucl. Med. Biol.* **21,** 819–825.
18. Guillaume M., Luxen A., Nebeling B., Argentini M., Clark J. C. and Pike V. W. (1991) Recommendations for fluorine-18 production. *Appl. Radiat. Isot.* **42,** 749–762.
19. Hajri A., Bruns C., Marbach P., Aprahamian M., Longnecker D. S. and Damgé C. (1991) Inhibition of the growth of transplanted rat pancreatic acinar carcinoma with octreotide. *Eur. J. Cancer* **27,** 1247–1252.
20. Hinkle P., Perone M. and Schonbrunn A. (1981) Mechanism of thyroid hormone inhibition of thyrotropin-releasing hormone action. *Endocrinology* **108,** 199.
21. de Jong M., Bakker W. H., Breemann W. A. P., van der Pluijm M. E., Kooij P. P. M., Visser T. J. *et al.* (1993) Hepatobiliary handling of iodine-125-Tyr^3-octreotide and indium-111-DTPA-D-Phe^1-octreotide by isolated perfused rat liver. *J. Nucl. Med.* **34,** 2025–2030.
22. Kimura N., Hayafuji C. and Kimura N. (1989) Characterization of 17-β-estradiol-dependent and -independent somatostatin receptor subtypes in rat anterior pituitary. *J. Biol. Chem.* **264,** 7033.
23. Krenning E. P., Bakker W. H., Kooij P. P. M., Breeman W. A. P., Oei H. Y., de Jong M. *et al.* (1992) Somatostatin receptor scintigraphy with

In-111-DTPA-D-Phe-1-octreotide in man: Metabolism, dosimetry and comparison with Iodine-123-Tyr-3-octreotide. *J. Nucl. Med.* **33,** 652–658.
24. Krenning E. P., Kwekkeboom D. J., Bakker W. H., Breeman W. A. P., Kooij P. P. M., Oei H. Y. *et al.* (1993) Somatostatin receptor scintigraphy with [^{111}In]-DTPA-D-phe^1] and [^{125}I-Tyr^3]-octreotide: The Rotterdam experience with more than 1000 patients. *Eur. J. Nucl. Med.* **20,** 716–731.
25. Lamberts S. W. J., Krenning E. P. and Reubi J. C. (1991) The role of somatostatin and its analogs in the diagnosis and treatment of tumors. *Endocr. Rev.* **12,** 450–482.
26. Lemaire M., Azira M., Dannecker R., Marbach P., Schweitzer A. and Maurer G. (1989) Disposition of sandostatin, a new synthetic somatostatin analogue in rats. *Drug Metab. Dispos.* **17,** 699–703.
27. Maina T., Stolz B., Albert R., Bruns C., Koch P. and Mäcke H. (1994) Synthesis, radiochemistry and biological evaluation of a new somatostatin analogue (SDZ 219-387) labelled with technetium-99m. *Eur. J. Nucl. Med.* **21,** 437–444.
28. Moi M. K. and Meares C. F. (1988) The peptide way to macrocyclic bifunctional chelating agents: Synthesis of 2-(*p*-Nitrobenzyl)-1,4,7,10-tetraazacyclododecane *N,N′,N″,N‴*-tetraacetic acid and study of its yttrium(III) complexes. *J. Am. Chem. Soc.* **110,** 6266–6267.
29. Morel G., Pelletier G. and Heisler S. (1986) Internalization and subcellular distribution of radiolabelled somatostatin-28 in mouse anterior pituitary tumor cells. *Endocrinology* **119,** 1972–1979.
30. Morel G. (1994) Internalization and nuclear localization of peptide hormones. *Biochem. Pharmacol.* **47,** 63–76.
31. Mentlein R., Buchholz C. and Krisch B. (1989) Binding and internalization of gold-conjugated somatostatin and growth hormone-releasing hormone in cultured rat somatotropes. *Cell. Tissue Res.* **258,** 309.
32. Najafi A. and Peterson A. (1993) Prepararation and *in vitro* evaluation of n.c.a. ^{18}F-labeled biotin. *Nucl. Med. Biol.* **20,** 401–405.
33. Quadri S. M., Vriesendorp H. M., Leichner P. K. and Williams J. R. (1993) Evaluation of indium-111- and yttrium-90-labeled linker-immunoconjugates in nude mice and dogs. *J. Nucl. Med.* **34,** 938–945.
34. Reichlin S. (1983) Somatostatin: First of two parts. *N. Engl. J. Med.* **309,** 1495–1501.
35. Reichlin S. (1983) Somatostatin: Second of two parts. *N. Engl. J. Med.* **309,** 1556–1563.
36. Rösch F., Qaim S. M. and Stöcklin G. (1993) Nuclear data relevant to the production of the positron emitting radioisotope ^{86}Y via the ^{86}Sr(*p*,*n*)- and ^{nat}Rb(^{3}He,xn)-processes. *Radiochimica Acta* **61,** 1–8.
37. Rösch F., Qaim S. M. and Stöcklin G. (1993) Production of the positron emitting radioisotopes for nuclear medical application. *Appl. Radiat. Isot.* **44,** 677–681.
38. Rota Kops E., Herzog H., Schmid A., Holte S. and Feinendegen L. E. (1990) Performance characteristics of an eight-ring whole-body PET scanner. *J. Assist Comput. Tomogr.* **14,** 437–445.
39. Sakamoto C., Goldfine I. D. and Williams J. A. (1984) The somatostatin receptor on isolated pancreatic acinar cell plasma membranes. *J. Biol. Chem.* **15,** 9623.
40. Schonbrunn A. (1982) Glucocorticoids down-regulate somatostatin receptors on pituitary cells in culture. *Endocrinology* **110,** 1147.
41. Seelig J., Nebel S., Ganz P. and Bruns C. (1993) Electrostatic and nonpolar peptide-membrane interactions: Lipid binding and functional properties of somatostatin analogues of charge $z = +1$ to $z = +3$. *Biochemistry* **32,** 9714–9721.
42. Smith-Jones P. M., Stolz B., Bruns C., Albert R., Reist H. W., Fridrich R. and Mäcke H. R. (1994) Gallium-67/gallium-68-[DFO]-octreotide—A potential radiopharmaceutical for PET imaging of somatostatin receptor-positive tumors: Synthesis and radiolabeling in vitro and preliminary in vivo studies. *J. Nucl. Med.* **35,** 317–325.
43. Srkalovic G., Cai R. Z. and Schally A. V. (1990) Evaluation of receptors for somatostatin in various tumors using different analogs. *J. Clin. Endocrinol. Metab.* **70,** 661–669.
44. Maina T., Stolz B., Albert R., Nock B., Bruns C. and Mäcke H. (1995) Synthesis, radiochemical and biological evaluation of ^{99m}Tc[N4-(D)phe^1]octreotide, a new derivative with high affinity for somatostatin receptors. *In: Technetium and Rhenium in Chemistry and Nuclear Medicine* (Edited by Nicolini M., Bandoli G. and Mazzi U.), pp. 395–400. Cortina International, Raven Press, New York.
45. Stolz B., Smith-Jones P., Ruser G., Albert R., Briner U., Weckbecker G. *et al.* (1994) Somatostatin analogues for radiodiagnosis and radiotherapy of cancer. *EUFEPS Symposium on Tumour Targeting with Radiolabelled Hormones and Antibodies.* Symposium abstract, Nuremberg, Germany.
46. Vaidyanathan G. and Zalutsky M. R. (1992) Labeling proteins with fluorine-18 using *N*-succinimidyl 4-[^{18}F]fluorobenzoate. *Nucl. Med. Biol.* **19,** 275.
47. Wester H. J., Hamacher K. and Stöcklin G. (1994) Tumour targeting with ^{18}F-labeled peptides and proteins: Comparative evaluation of five different ^{18}F-labeling agents. *EUFEPS Symposium on Tumour Targeting with Radiolabelled Hormones and Antibodies.* Symposium abstract, Nuremberg, Germany.